# *Development of an Ultra-Narrow-Linewidth Laser for Interrogating the $^1S_0 - {}^3P_0$ Clock Transition in Yb atoms*

Kazumoto Hosaka [1, 2], Masami Yasuda [1, 2], Hajime Inaba [1, 2], Takuya Kohno [2], Yoshiaki Nakajima [1, 3], Atsushi Onae [1], and Feng-Lei Hong [1, 2]

[1] National Metrology Institute of Japan (NMIJ), National Institute of Advanced Industrial Science and Technology (AIST), Tsukuba Central 3, Ibaraki 305-8563, Japan

[2] CREST, Japan Science and Technology Agency, 4-1-8 Honcho Kawaguchi, Saitama 332-0012, Japan

[3] University of Fukui, 3-9-1 Bunkyo, Fukui, 910-8507, Japan

kazu.hosaka@aist.go.jp

***Abstract*— A light source to drive the $^1S_0 - {}^3P_0$ transition in Yb atoms is generated by two solid state lasers: a Nd:YAG laser and a Yb:YAG laser, using a sum-frequency generation (SFG) scheme. With a ridge waveguide (WG) periodically poled lithium niobate (PPLN) device, SFG power of about 150 mW is obtained at the required frequency. The performance of the clock laser system is evaluated with studies of frequency stability measured by an optical frequency comb and with atomic absorption spectra of the $^{171}$Yb clock transition at 578 nm.**

## I. INTRODUCTION

Optical clocks based on forbidden transitions in either laser cooled single ions or neutral atoms are currently being developed worldwide and offer a new level of time-keeping accuracy. The spin forbidden transitions in trapped neutral atoms, such as Sr, Yb, and Hg, using optical lattice technique [1, 2], have a great potential to be an extremely accurate optical frequency standard. The $^1S_0 - {}^3P_0$ transition in Sr was already chosen to be one of 'the secondary representations of the second' [3]. The same transition in Yb is also an excellent candidate for an optical frequency standard [4, 5]. Using even isotope $^{174}$Yb, the absolute frequency of the $^1S_0 - {}^3P_0$ clock transition was determined with an uncertainty of 0.8 Hz already [6].

At NMIJ, we have been developing an Yb optical lattice clock [7], because of several advantages as follows: 1) low nuclear spin in the odd isotopes; 2) a relatively large range of abundant isotopes; and 3) room temperature black body radiation shift is about half of that of Sr. The $^3P_0$ state in Yb has a long life time of approximately 20 s and the corresponding natural linewidth of the $^1S_0 - {}^3P_0$ transition is about 10 mHz. The stability of a frequency standard based on this transition will not be limited by the natural linewidth, but only by the linewidth of the clcok laser and the stability of external perturbations. A light source generated by a Nd:YAG laser and a Yb fibre laser using a SFG scheme had been developed for the Yb clock transition at 578 nm [8]. Recently we have employed a Yb:YAG laser with a monolithic cavity instead of the Yb fibre laser due to relatively narrow linewidth and small jitter of the light source. This paper reports on recent progress in the development of the probe laser which drives the $^1S_0 - {}^3P_0$ transition in Yb atoms confined in an optical lattice trap.

## II. EXPERIMENTAL

A schematic of the probe laser system including frequency stabilization is shown in Fig. 1. Light at 578 nm is generated by a Nd:YAG laser and a Yb:YAG laser using a SFG scheme. Fundamental lights from the Nd:YAG laser at 1319 nm and the Yb:YAG laser at 1030 nm are delivered to a ridge waveguide (WG) periodically poled lithium niobate (PPLN) device via a wavelength division multiplexing (WDM) coupler. The temperature of the PPLN is optimized to maximize the out-put power at 578 nm. Figure 2 shows typical relation between optical power of the SFG at 578 nm and temperature of the PPLN. In this case, IR input power to optical fibres at 1030 nm and 1319 nm were about 288 mW and 419 mW, respectively. Considering power loss of the fibre couplings, fibre transmissions and fibre connections, effective IR powers delivered into the PPLN are estimated to be less than 50 % of the IR input power mentioned above.

The laser frequency at 578 nm is locked by the Pound-Drever-Hall (PDH) technique to a $TEM_{00}$ mode of an etalon by feedback to a piezoelectric transducer bonded to the laser crystal in the Nd:YAG. A local oscillator at about 2.5 MHz drives the electro-optics modulator (EOM) putting sidebands on the light. A high finesse (F ~ 400000±150000) Fabry – Pérot etalon made from ultra low expansion (ULE) glass with a spacer of 75 mm and a diameter of 25.4 mm is mounted vertically [9] in an aluminium vacuum chamber at a pressure of 3 $\times 10^{-5}$ Pa. Using silicon RTV, the optical cavity was

978-1-4244-3510-4/09/$25.00  

bonded to an aluminium disc, which is supported by three Teflon posts. The system has two layers of temperature control. One is on the aluminium vacuum chamber and another one on a copper box that surrounds it. The temperature controller on the vacuum chamber works on the principle of applying ac across opposite corners of a Wheatstone bridge, which incorporates a thermistor. A lock-in amplifier measures the voltage across the other two corners of the bridge and its output is used as an error signal, resulting it controls the temperature to within a few mK.

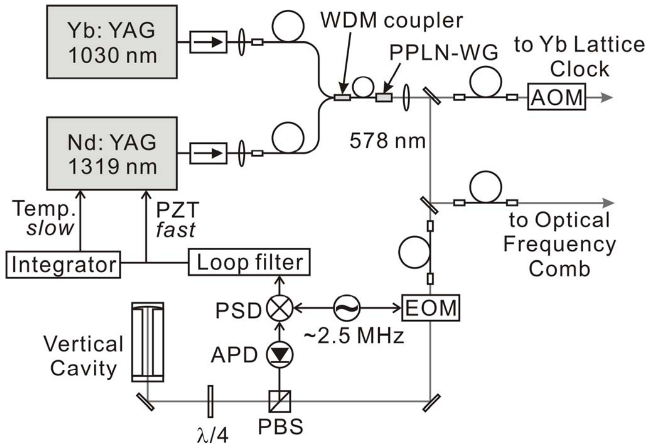


Figure 1. A schematic diagram of the optics and electronics required for frequency stabilization of the probe laser. EOM, electro-optic-modulator; AOM, acousto-optic-modulator; PBS, polarizing beam splitter; APD, avalanche photodiode.

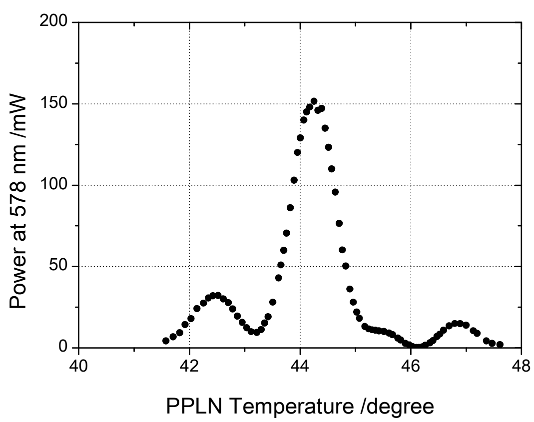


Figure 2. Out put power at 578nm from the PPLN-WG as a function of PPLN temperature. In this measurement, IR input power to optical fibres at 1030 nm and 1319 nm were 288 mW and 419 mW, respectivily. Considering power loss of the fibre couprings, fibre transmissions and fibre conections, effective IR powers delivered into the PPLN are estimated to be less than 50 % of the input power.

The vacuum chamber is now supported on a passive vibration isolation platform which will be situated within an acoustic isolation box. Measurements of the vibration levels in our laboratory at NMIJ have been made. The root spectral density of the vertical acceleration on the floor is approximately $5\times10^{-5}$ $ms^{-2}/\sqrt{Hz}$ in the frequency range from 1 to 100 Hz. Therefore, it is expected that $1\times10^{-6}$ $ms^{-2}/\sqrt{Hz}$ can be achieved on the vibration isolation platform.

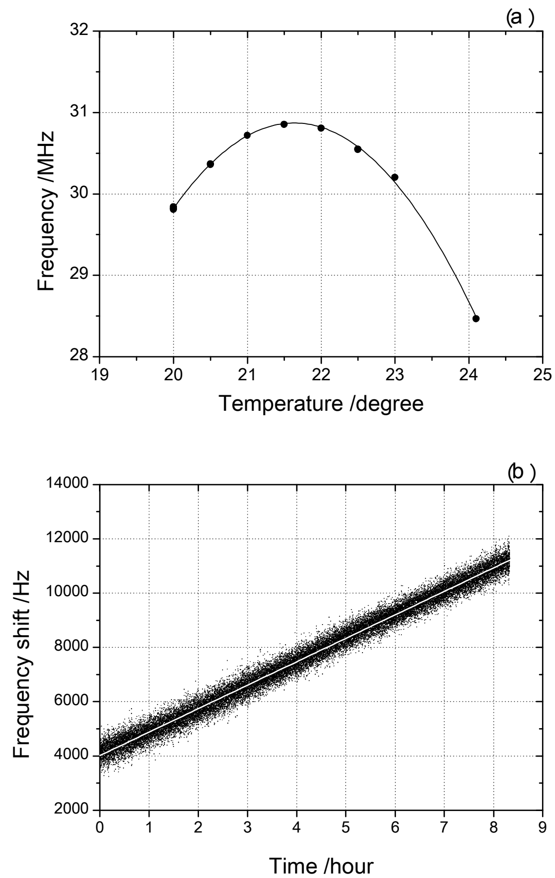


Figure 3. (a) ULE cavity frequency as a function of the vacuum chamber wall temperature at thermal equilibrium conditions. The solid curve is a fit to the data. The coefficient of thermal expansion is zero at about 26.1°C. (b) Frequency of the reference ULE cavity as a function of time. Frequency measured using a fibre comb referenced to a hydrogen maser source. The observed ULE cavity drift rate is about 240 mHz/s.

ULE glass has a temperature where the coefficient of thermal expansion crosses zero. To determine the zero crossing temperature of the cavity, the resonant frequencies of the cavity were measured by an optical frequency comb based on a mode-locked fibre laser (fibre comb) [10] as a function of the vacuum chamber wall temperature at thermal equilibrium conditions (Fig. 2 (a)). In Fig. 2 (a), the dots indicate beat frequencies between the comb and the clock laser at averaging time of ~ 100 s typically. From a fitting curve to the data points, the coefficient of thermal expansion is zero at the extremum found at around 26.1°C. After setting the vacuum chamber temperature at 21.6°C, the long term drift rate of the resonant frequency was measured by the optical fibre comb referenced to a hydrogen maser source, as shown in Fig. 2(b). The dots represent beat frequencies between the comb and the clock laser with 1 s gate time on a dead-time-free counter. Scatter of the dots is mainly due to frequency fluctuation of the hydrogen maser. The solid line corresponds to a linear fit through data point, indicating the frequency drift of about 240 mHz/s, which is mainly attributed for the creep effect.

## III. RESULTS AND DISCUSSION

To evaluate the performance of the clock laser, first we investigated frequency stability using a fibre comb referenced to a cryogenic Sapphire oscillator [11]. The linewidth of the laser was then estimated by spectroscopy of the clock transition in $^{171}$Yb atoms confined in a one-dimensional optical lattice.

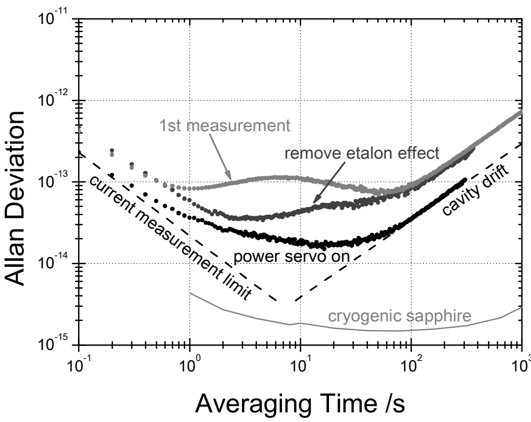


Figure 4. Fractional frequency stability (Allan deviation) as a function of averaging time measured by the fibre comb referenced to the cryogenic Sapphire oscillator.

Fractional frequency stability (Allan deviation) as a function of averaging time, which is measured by the fibre comb, is shown in Fig. 4. At the beginning of this experiment, the observed stability was at around $10^{-13}$ between 1 and 100 s (light grey dots in Fig. 4). This relatively high revel of the instability was due to an etalon effect, which accidentally existed on the beam pass. After removing the etalon effect, vacuum chamber temperature has been adjusted to the zero crossing temperature and a power servo system is employed to stabilise the incident laser power into the cavity. In Fig. 4, black dots represent the latest result, indicating about $2 \times 10^{-14}$ at 10 s. In the short averaging time region, we have a measurement limit that is in inverse proportion to the averaging time. We expect that photo detection used in the repetition rate stabilization mainly give the limitation. On the other hand, the frequency stability in the long averaging time is limited by the cavity drift. One can see that the stability of the clock laser does not reach to these limits at averaging time between 0.5 and 50 s, indicating other instability effects. To improve the performance of the system, it will be necessary to evaluate the variation of residual amplitude modulation (RAM) and need to minimize the RAM. It would be required further isolation of the cavity from vibrations, and this may be achieved by optimizing the hold position of the vertical cavity to the centre of mass exactly, where vibrations does not play a large role in changing the length of the cavity. Furthermore, the acoustic enclosure that has a relatively good isolation of ~ -20 dB in the infrasound range will be installed in near future.

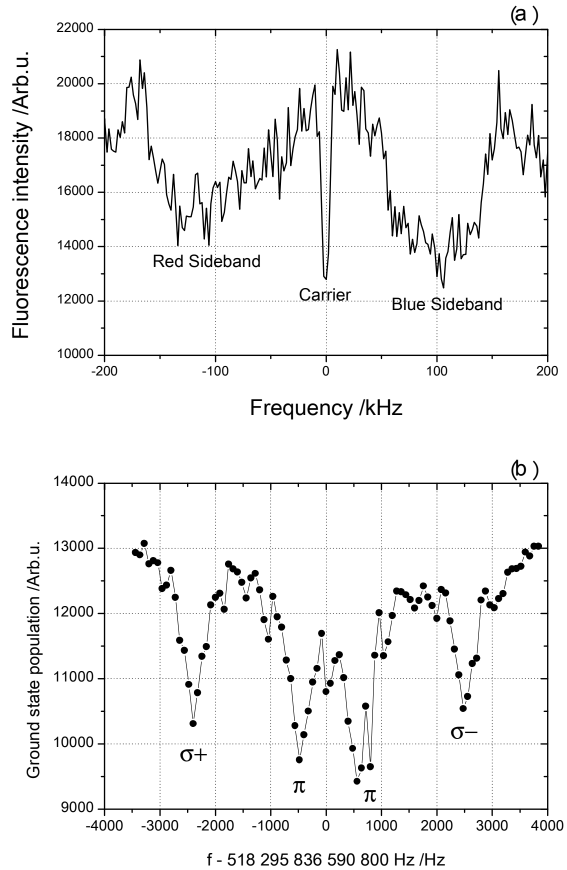


Figure 5. A spectroscopy of $^{171}$Yb atoms in a one dimensional lattice. (a) A narrow carrier at the centre and red (lower) and blue (higher) vibrational sidebands of the $^{171}$Yb atoms in the lattice are shown. (b) A spectrum of $^{171}$Yb isotope in a magnetic field showing the four possible transitions between Zeeman substates. The observed linewidth of the transition is limited by a power broadening effect.

Spectroscopy of the $^1S_0 - {}^3P_0$ transition in $^{171}$Yb atoms trapped in an optical lattice is performed using the electron shelving technique, as shown in Fig. 5. Details of the experimental arrangement and procedure to trap ultra cold neutral Yb atoms in the optical lattice are described in [7], so here we will only mention the spectroscopy that has been made. Spectral lineshapes of the clock transition are obtained by a controlled scan of the double-passed AOM that bridges the offset between the cavity resonant frequency and the transition frequency in $^{171}$Yb. The spectrum shown in Fig. 5(a) is the average of three scans where the AOM was stepped 300 times for the total scan range of 400 kHz. When the clock laser frequency repeatedly scanned over the transition using the AOM, fluorescence level, which is proportional to the ground level population, is recorded in a computer. Figure 5(a) shows a narrow carrier at the centre and red (lower) and blue (higher) vibrational sidebands of the $^{171}$Yb atoms in the lattice.

We have observed the Zeeman components by doing the spectroscopy in a homogeneous magnetic field. In the case of $^{171}$Yb, four transitions can be observed: 2 $\pi$ polarized transitions between the same $m_F = \pm 1/2$ Zeeman sublevels, and $\sigma+$, $\sigma-$ polarized transitions between the different $m_F = \pm 1/2$ Zeeman sublevels. Figure 5 (b) shows an average data set made up of ~ 120 separate scans each consisting of 50 steps in the offset frequency of 80 Hz. Before these scans are collated, the absolute frequency of the each data point has been determined to remove the cavity drift. The collated data gives the Zeeman component profile and narrow linewidths are observed, having a width of a few hundred Hz. For the measurement, the clock laser power intensity was about 2.3 mW/cm$^2$ and the observed linewidths of the transition are limited by a power broadening effect. Therefore, one can say that the clock laser linewidth is less than the absorption linewidth at least.

## IV. Summary

A clock laser to drive the $^1S_0 - {}^3P_0$ transition in Yb atoms has developed based on the SFG scheme with the Nd:YAG laser and the Yb:YAG laser. SFG power of about 150 mW is obtained at the required frequency. The frequency stability of the clock laser was measured using the fibre comb referenced to the cryogenic Sapphire oscillator. After several improvements, the stability is now about $2 \times 10^{-14}$ at the averaging time of 10 s, which is, however, 10 time higher than the current measurement limit. Spectroscopy of the clock transition in $^{171}$Yb atoms is successfully achieved. From observed Zeeman components, the clock laser linewidth is estimated to be less than a few hundred Hz. To achieve reductions in clock laser linewidth towards 1 Hz, investigation on the RAM variation in the locking system would be required. It is also important to find the best support position of the vertical cavity where the length of the cavity is insensitive to vibrations. An acoustic enclosure will be prepared to isolate the cavity from acoustic noise in the infrasound range. We expect that the high-stability of about $1\times10^{-15}$ can be achieved, which is mainly limited by thermal noise in the reference cavity used for frequency stabilization of the laser [12]. A second ULE cavity at 578 nm is currently being constructed to allow evaluation of linewidth of the lights by comparing two identical systems to be performed.

## Acknowledgment

We are grateful to K. Watabe for his work on the cryogenic Sapphire oscillator. We also thank J. Yumoto and Y. Nishida for providing the ridge WG-PPLN.

## References

[1] H. Katori, “Spectroscopy of strontium atoms in the Lamb-Dicke confinement”, Proceedings of the 6th Symposium on Frequency Standards and Metrology, P. Gill, ed., World Scientific, Singapore, pp. 323, 2002.

[2] M. Takamoto, F. -L. Hong, R. Higashi, and H. Katori, “An optical lattice clock”, Nature, vol. 435, no. 7040, pp. 321, May 2005.

[3] CIPM (International Committee for Weights and Measures) recommendation, October 2006.

[4] S. G. Porsev, A. Derevianko, and E. N. Fortson, “Possibility of an optical clock using the 6 $^1S_0$ – 6 $^3P_0$ transition in $^{171,173}$Yb atoms held in an optical lattice”, Phys. Rev. A, vol. 69, pp. 021403(R), Februaly 2004.

[5] C. W. Hoyt, Z. W. Barber, C. W. Oates, T. M. Fortier, S. A. Diddams, and L. Hollberg, “Observation and Absolute Frequency Measurements of the $^1S_0$ – $^3P_0$ Optical Clock Transition in Neutral Ytterbium”, Phys. Rev. Lett., vol. 95, pp.083003, August 2005.

[6] N. Poli, Z. W. Barber, N. D. Lemke, C. W. Oates, L. S. Ma, J. E. Stalnaker, I. M. Fortier, S. A. Diddams, L. Hollberg, J. C. Bergquist, A. Brusch, S. Jefferts, I. Heavner, and I. Parker, “Frequency evaluation of the doubly forbidden $^1S_0$ – $^3P_0$ transition in bosonic $^{174}$Yb”, Phys. Rev., A vol. 77, pp. 050501(R), May 2008.

[7] M. Yasuda, F.-L. Hong, T. Kohno, H. Inaba, K. Hosaka, C. Willis, T. Kurosu, A. Onae, and S. Ohshima, “Present status of the development of an Yb optical lattice clock at NMIJ/AIST”, in Time and Frequency Metrology, Proceedings of SPIE, R. Jason Jones, ed., vol. 6673, article CID no. 6673 0D, 2007.

[8] F.-L. Hong, H. Inaba, K. Hosaka, M. Yasuda, and A. Onae, “Doppler-free spectroscopy of molecular iodine using a frequency-stable light source at 578 nm”, Optics Express, vol.17, pp.1652-1659, Febuary 2009.

[9] M. Notcutt, L.-S. Ma, J. Ye, and J. L. Hall, “Simple and compact 1-Hz laser system via an improved mounting configuration of a reference cavity”, Optics Letters, vol. 30, no. 14, pp. 1815-1817, July 2005.

[10] H. Inaba, Y. Daimon, F. L. Hong, A. Onae, K. Minoshima, T. R. Schibli, H. Matsumoto, M. Hirano, T. Okuno, M. Onishi, and M. Nakazawa, "Long-term measurement of optical frequencies using a simple, robust and low-noise fiber based frequency comb," Optics Express, vol. 14, pp. 5223-5231, Jun 2006.

[11] K. Watabe, J. G. Hartnett, C. R. Locke, G. Santarelli, S. Yanagimachi, T. Shimazaki, T. Ikegami, and S. Ohshima, “Short Term Frequency Stability Tests of Two Cryogenic Sapphire Oscillators”, Jpn. J. Appl. Phys., vol. 45, no. 12, pp. 9234–9237, December 2006.

[12] K. Numata, A. Kemery, and J. Camp, “Thermal-noise limit in the frequency stabilization of lasers with rigid cavities”, Phys. Rev. Lett., vol. 93, no. 25, pp. 250602, December 2004.